

# Lawrence Berkeley National Laboratory

## Recent Work

**Title**

NEUTRAL-BEAM DESIGN OPTIONS

**Permalink**

<https://escholarship.org/uc/item/1z73d98w>

**Author**

Stearns, J.W.

**Publication Date**

1976-04-01

0 0 0 0 4 4 0 0 3 2 1

Presented at the Technology of Controlled  
Nuclear Fusion Conference, Richland, WA,  
September 21 - 23, 1976

LBL-4492

c.1

NEUTRAL-BEAM DESIGN OPTIONS

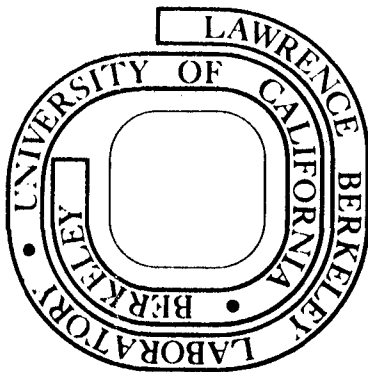
J. W. Stearns, K. H. Berkner, and R. V. Pyle

April 1976

Prepared for the U. S. Energy Research and  
Development Administration under Contract W-7405-ENG-48

**For Reference**

Not to be taken from this room



LBL-4492

c.1

## **DISCLAIMER**

This document was prepared as an account of work sponsored by the United States Government. While this document is believed to contain correct information, neither the United States Government nor any agency thereof, nor the Regents of the University of California, nor any of their employees, makes any warranty, express or implied, or assumes any legal responsibility for the accuracy, completeness, or usefulness of any information, apparatus, product, or process disclosed, or represents that its use would not infringe privately owned rights. Reference herein to any specific commercial product, process, or service by its trade name, trademark, manufacturer, or otherwise, does not necessarily constitute or imply its endorsement, recommendation, or favoring by the United States Government or any agency thereof, or the Regents of the University of California. The views and opinions of authors expressed herein do not necessarily state or reflect those of the United States Government or any agency thereof or the Regents of the University of California.

## NEUTRAL-BEAM DESIGN OPTIONS\*

J. W. Stearns, K. H. Berkner, and R. V. Pyle

LAWRENCE BERKELEY LABORATORY

The designs and costs of magnetic-confinement experimental devices and reactors can be affected strongly by the choice of parameters for the neutral-beam injection system. To provide the designer with information with which to estimate the physical and cost consequences of variations in energy, neutralizer thickness, ion-species mixtures, etc., we are carrying out parametric studies of the neutralization efficiency. Some of the results are reported here. The data base is too small and uncertain to permit calculations which would optimize all aspects of designs at this time.

INTRODUCTION

The designs and costs of magnetic-confinement experimental devices and reactors that use neutral injection for heating and/or fueling can be affected strongly by the choice of parameters used in the neutral-injector design. For example, the development and construction of the neutral-injection systems for the TFTR tokamak<sup>(1)</sup> and the MX mirror<sup>(2)</sup> experiments account for roughly one-half of the total hardware costs. Thus, the consequence of a relatively small design change may amount to several million dollars.

As neutral-beam-system developers, we are asked such questions as: "What will happen if the length of the neutralizer is decreased?," or, "What research and development efforts are most important to the injector development program?" Unfortunately, there are very few reliable data on such important topics as gas efficiencies or atomic-ion fractions attainable in the ion source of an injector. As a result, we must base our calculations on plausible values for these quantities. Much more research should be done in these areas.

The data base is much better for atomic and molecular collision processes. The work reported here is concerned with the consequences of these collisions, when different assumptions are made about neutralizer thickness, atomic-and molecular-ion-species mixtures in the plasma source, electrostatic-energy-recovery efficiency, and collision cross sections.

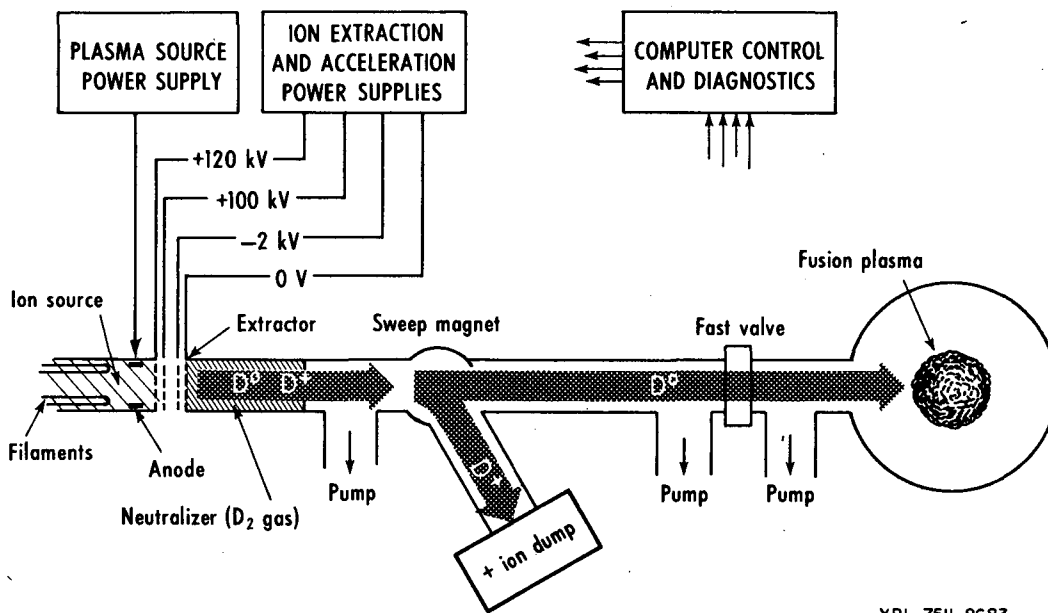
This paper is an extension of a previous report<sup>(3)</sup> which gives some of the motivation and physics in more detail. In particular, we show

1. The effects of changing the neutralizer thickness (molecules/cm<sup>2</sup>) on the production of 20- to 400-keV deuterium-atom beams,
2. The effects of changing the ion-species current mixtures in the accelerated beam from  $D^+ : D_2^+ : D_3^+ = 60:20:20$  to  $90:7:3$ , with and without recovery of the kinetic energy of charged particles emerging from the neutralizer.

For simplicity, we concentrate mainly on injectors in which positive atomic- and molecular-ions are accelerated and then partially neutralized in D<sub>2</sub> gas; we also show some results for D<sup>-</sup> beams. As an

---

\*Work done under the auspices of the U.S. ERDA.



XBL 7511-8683

FIGURE 1. Schematic diagram of a beam line for a neutral injection system.

example, we will consider some aspects of the TFTR beam line design.<sup>(4)</sup>

We will appreciate suggestions, e.g. improvements in the cross sections used in our calculations, and will be happy to supply data in numerical form or compute neutral yields, etc., for specific applications.

BEAM SPECIES AND NEUTRALIZATION

In a typical neutral-beam system, slow ions, produced in an electric discharge, are accelerated to the desired energy, and the energetic ions are converted to energetic atoms or molecules by collisions in a neutralizer cell (Fig. 1). In a deuterium (hydrogen or tritium) discharge the slow ions exist principally in four forms, namely  $D^+$ ,  $D_2^+$ ,  $D_3^+$ , and  $D^-$ . Some of these ions, when accelerated, can be electrically neutralized by capturing an electron from the neutral-gas target, by dissociation, or by losing an electron to the target. The competition between electron-capture-and-loss collisions establishes a mixture of positive, negative, and neutral particles in

the emerging beam. When the incident ion-beam consists of  $D^+$  or  $D^-$ , all constituents of the emerging beam have the same energy as the incident ions; however, incident  $D_2^+$  ( $D_3^+$ ) ions of energy  $E$  will result in beams containing neutral particles of energy  $E$  and  $1/2 E$  ( $2/3 E$  and  $1/3 E$  for  $D_3^+$ ). The various collision products are illustrated in Fig. 2.

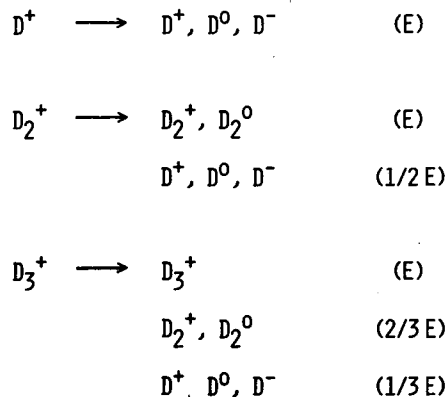


FIGURE 2. Beam constituents resulting when ions of energy  $E$  (on the left) pass through a neutralizer cell. The resultant particle energies are indicated in parentheses.

The equations that describe the populations of the various beam constituents as a function of the neutralizer thickness have been presented in Reference 3, where it was shown that sixteen different cross sections must be known to describe the populations at a given energy and for a given neutralizer gas. In our earlier paper we tabulated the relevant cross sections, obtained from the literature, for  $D_2$  targets. Since then we have adjusted some of the cross-section values (within their stated uncertainties) to make our calculated results more consistent with equilibrium measurements.<sup>(5)</sup> The cross-section values used for the calculations in the present paper are listed in Table I. They are not

to be considered "best values," i.e. no evaluations of the various experiments have been made. We are continually updating this table as more reliable cross-section values become available and as inconsistencies in the results become obvious.

We have concentrated on  $D_2$  targets because the required cross sections are not always available for an arbitrary choice of neutralizers. Enough sample calculations have been carried out, however, to indicate that  $D_2$  is representative of the better gas neutralizers. Other gases such as  $N_2$  or Ar, do not yield radically different neutralization efficiencies, although the maximum efficiency can usually be obtained at lower gas-target thicknesses. Thus other

TABLE I. Cross-sections used in the calculations ( $10^{-17} \text{cm}^2/D_2$  molecule). Most entries were obtained from measurements in  $H_2$  gas with hydrogen projectiles of one-half the tabulated energies. Estimated uncertainties are as shown under each column except as noted. Parentheses indicate extrapolations or interpolations where no uncertainty can be assigned.  $\sigma_{ij}$  ( $i, j = 1, 0, -1$ ) indicates cross section for change from charge state  $i$  to  $j$ .  $\sigma_{D^0}$ ,  $\sigma_{D^+}$ , etc. symbolize cross sections for the production of  $D^0$ ,  $D^+$ , etc.

Ion Energy keV	$D^+$		$D^0$		$D^-$		$D_2^+$			$D_2^0$			$D_3^+$			
	$\sigma_{10}$	$\sigma_{1-1}$	$\sigma_{01}^{(a)}$	$\sigma_{0-1}$	$\sigma_{-10}$	$\sigma_{-11}$	$\sigma_{D_2^0}$	$\sigma_{D^+}$	$\sigma_{D^0}$	$\sigma_{D_2^+}$	$\sigma_{D^+}$	$\sigma_{D^0}^{(b)}$	$\sigma_{D_2^+}$	$\sigma_{D^0}$	$\sigma_{D^+}$	$\sigma_{D^0}$
20	83	0.46	9.0	2.4	109	8.9	46	21	75	7.8	3.4	25	9.6	31	8.4	58
40	59	1.00	12.9	1.9	94	9.0	36	22	83	11.9	5.3	19.8	11.9	38	12.7	81
80	25.5	0.26	16.0	0.98	71	8.4	21	24	71	17.0	6.8	12.8	12.4	42	17.7	96
120	11.0	0.03	13.9	0.52	58	7.3	12	24	55	20	7.2	10.0	11.6	35	20.2	91
160	5.0	0.0055	12.0	0.30	50	6.3	7.0	24	47	20	7.1	8.5	10.7	28	22	79
200	2.4 <sup>(c)</sup>	0.0017	10.7	(0.19)	44	(5.4)	4.4	24	34 <sup>(d)</sup>	20	6.9	7.5	9.8	21	23	69
240	1.24 <sup>(c)</sup>	0.00045	9.7	(0.12)	39	(4.8)	2.8	23	27 <sup>(d)</sup>	18.6	6.7	6.7	9.0	15.7	24	60
400	0.17 <sup>(c)</sup>	(0)	7.0	(0.028)	29	(2.9)	0.70	19	13 <sup>(d)</sup>	15.1	5.8	5.1	7.1	4.8	24	37
600	0.02 <sup>(c)</sup>	(0)	5.1	(0.007)	22	(1.7)	(0.175)	15	7.2 <sup>(d)</sup>	11.8	4.9	4.1	5.6	1.58	23	26
800	0.0055	(0)	4.0	(0.0024)	18	(1.04)	(0.090)	12.3	5.0 <sup>(d)</sup>	9.6	4.3	3.5	4.7	0.73	21	20
1000	0.0017	(0)	3.3	(0.0011)	15	(0.69)	(0.045)	10.3	3.8 <sup>(d)</sup>	8.0	3.7	3.1	4.0	0.41	19	17
Estimated uncertainties	±10%	±30%	±10%	±20%	±15%	±10%	±10%	±20%	±10%	±20%	±25%	±25%	±15%	±20%	±10%	±10%

(a)  $\sigma_{01}$  adjusted to make calculated results consistent with  $F_0^\infty$  measurements.

(b) Reaction  $D_2^0 + D^0 + D^+$  only.

(c) ± 15%

(d) ± 20%

neutralizer choices could minimize the gas load on the system; they would, however, be a possible source of higher Z impurity for the fusion plasma.

A computer code has been written to numerically integrate the equations that describe the populations of the beam constituents (Ref. 3). The cross sections of Table I are stored in this code; the input parameters for the code are the beam energy  $E$  and the population mixture of the ion beam (e.g. 120 keV, 100%  $D^-$ ; 200 keV, 75%  $D^+$ , 15%  $D_2^+$ , 10%  $D_3^+$ ). The appropriate cross sections are determined by interpolation of the entries of Table I and the populations of all beam constituents ( $D^+$ ,  $D^0$ , and  $D^-$  at  $E$ ,  $1/2 E$ , and  $1/3 E$ ;  $D_2^0$  and  $D_2^+$  at  $E$  and  $2/3 E$ ; and  $D_3^+$  at  $E$ ) are obtained as a function of the target thickness  $\pi$  (molecules/cm<sup>2</sup>) by numerical integration.

We have not carried out a systematic error analysis by propagating the cross-section uncertainties through the calculations. We note, however, that the equilibrium- (thick-target)  $D^0$  fractions agree within about  $\pm 2\%$  with the measurements listed in the review article by Allison and Garcia-Munoz,<sup>(5)</sup> and that the growth curves for total-neutral-power production from  $D_2^+$  and  $D_3^+$  agree well with measurements reported by us at the higher energies.<sup>(6)</sup>

There is, of course, no single parameter that can fully summarize the results of these calculations; however, much of the information can be summarized with a parameter that we call the neutralization efficiency. In our earlier paper<sup>(3)</sup> we defined this as

$$\eta = \frac{(\text{power in neutral beam})}{(\text{power in initial ion beam})}; \quad [1]$$

in this definition all emerging neutrals, including molecules and fractional-energy

atoms, were included in determining the efficiency. For many design applications, however, only the atoms of the prescribed energy are of interest; the molecules and lower-energy atoms may be considered waste power because (a) they do not penetrate very deep into the target-plasma or (b) they dilute the tritium target-plasma. In the present paper, therefore, we use the efficiency for the production of atoms of the prescribed energy  $E$ , which is defined by

$$\eta' = \frac{(\text{power in atoms of energy } E)}{(\text{power in initial ion beam less recovered power, if any})}. \quad [2]$$

For a positive-ion beam containing a mixture of  $D^+$ ,  $D_2^+$ , and  $D_3^+$  of energy  $E$  only the "full-energy"  $D^0$  of energy  $E$  are included in the calculation of  $\eta'$ . For a "pure" beam of  $D_2^+$  of energy  $2E$  or  $D_3^+$  of energy  $3E$ ,  $\eta'$  is calculated for the  $D^0$  fragments of energy  $E$ , since these are the only atoms produced by collisions.

In Figures 3 and 4 we give examples of the neutralization efficiency  $\eta'$  vs  $D_2^-$ -target thickness for "pure" ion beams (100%  $D^-$ ,  $D^+$ ,  $D_2^+$ , or  $D_3^+$ ) for energies currently of interest to the MFE program. The energy label on each graph identifies the energy  $E$  of the resulting atom beam; e.g. to obtain 20-keV  $D^0$ , the appropriate ion beams would be 20-keV  $D^+$  or  $D^-$ , 40-keV  $D_2^+$ , or 60-keV  $D_3^+$ . Since the cross sections depend only on the relative velocity, the 20-keV- $D^0$  graph is also appropriate for 10-keV  $H^0$ . At energies above  $\sim 80$  keV/D the desirability of  $D^-$  beams is immediately obvious from the figures; not only do these have the largest conversion efficiency, but they also require less neutralizer thickness to attain maximum efficiency. (At very thick targets all beams reach collisional equilibrium and the distinction between

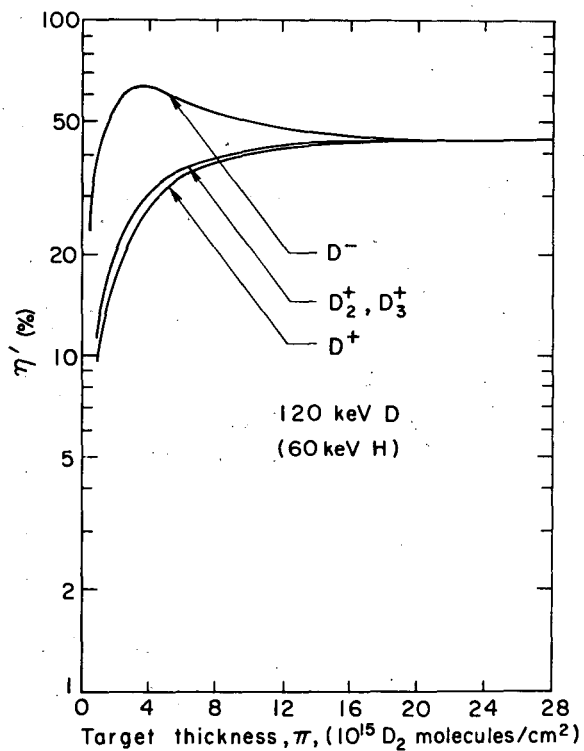
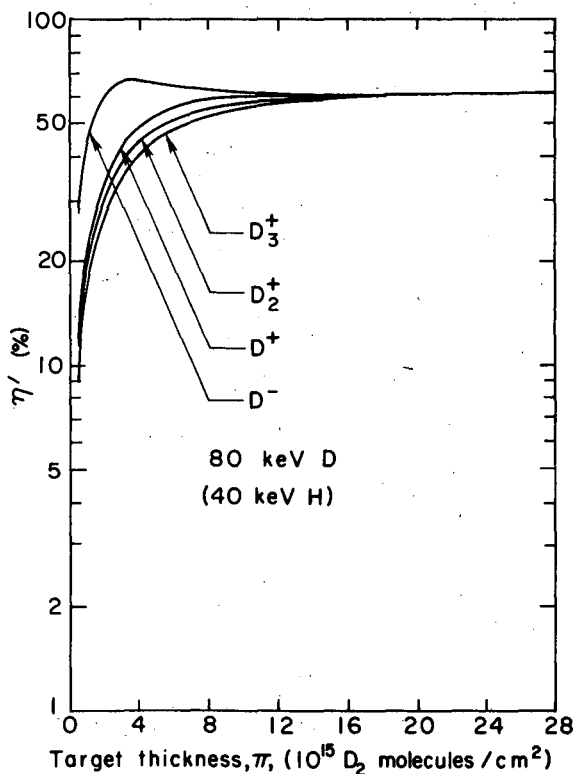
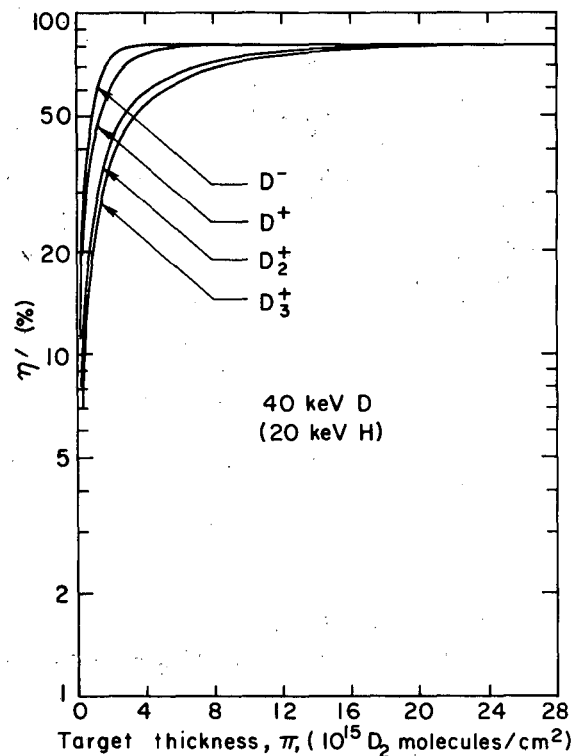
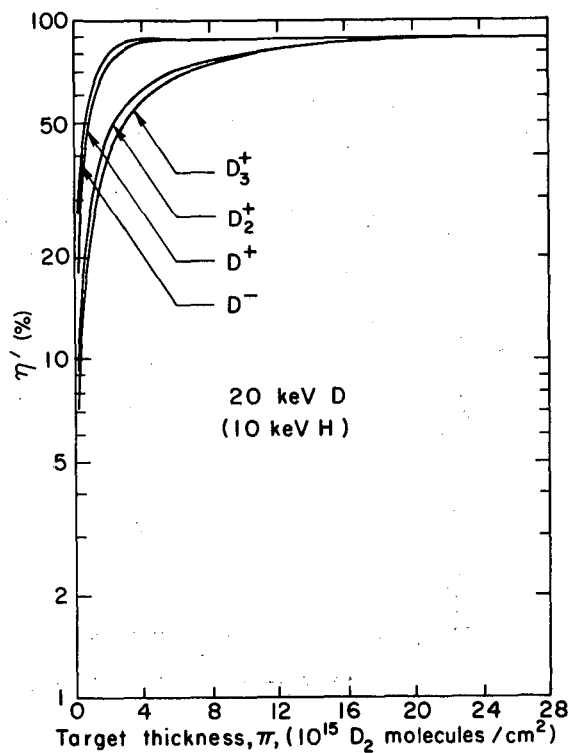


FIGURE 3. Neutralization efficiency,  $\eta'$ , (see equation [2]) vs  $D_2$ -neutralizer thickness for each of the four beams;  $D^+$ ,  $D_2^+$ ,  $D_3^+$ , and  $D^-$  at energies  $E$ ,  $2E$ ,  $3E$  and  $E$ , respectively, for energy  $E$  indicated on each diagram. (Equivalent hydrogen energy shown in parentheses.)



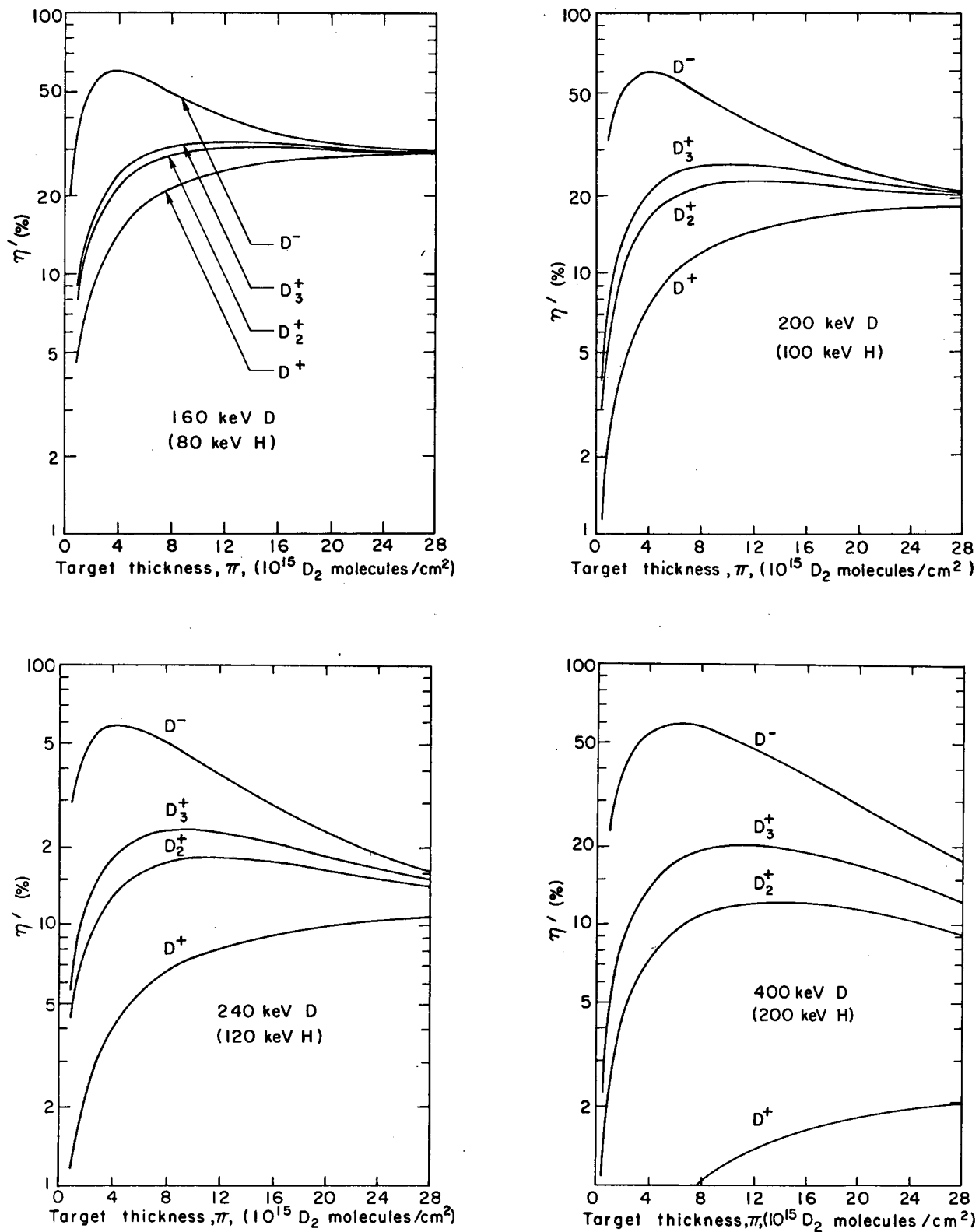


FIGURE 4. Neutralization efficiency,  $\eta'$ , (see equation [2]) vs D<sub>2</sub>-neutralizer thickness for each of the four beams; D<sup>+</sup>, D<sub>2</sub><sup>+</sup>, D<sub>3</sub><sup>+</sup>, and D<sup>-</sup> at energies E, 2E, 3E and E, respectively, for energy E indicated on each diagram. (Equivalent hydrogen energy shown in parentheses.)

the various initial beams disappears). It can also be seen from the figures that below  $\sim 40$  keV there is little difference between  $D^+$  and  $D^-$  beams, whereas  $D_2^+$  and  $D_3^+$  beams are undesirable because they require thicker targets [either higher pressures (which imply more pumping speed) or longer neutralizers (which mean longer beam lines)]. Around 120 keV/D the molecular ions begin to come into their own and have efficiencies comparable to those of  $D^+$ ; one must remember, however, that the "pure" molecular-ion beams require either twice or thrice the accelerating voltage. Above  $\sim 160$  keV/D molecular ions have a maximum in  $\eta'$  at intermediate target thicknesses; this is because the cross sections for dissociation are larger than those for electron capture, but the atoms resulting from dissociation are destroyed as the targets get thicker. Above  $\sim 200$  keV/D,  $D^+$  beams are no longer competitive with the others.

Figures 3 and 4 also indicate the difficulty in specifying the neutralizer target-thickness for a given situation. Except for  $D^-$  above  $\sim 80$  keV and the molecular ions above  $\sim 120$  keV/D, there is no distinct maximum in  $\eta'$  vs  $\pi$  -- only an approach to thick-target equilibrium. For discussion purposes we arbitrarily define the "optimum" neutralizer thickness as the value of  $\pi$  for which a maximum value of  $\eta'$  is obtained, if a significant maximum exists; otherwise it is the value of  $\pi$  required to achieve 95% of the equilibrium  $\eta'$ . For example, note that for 120-keV  $D^+$   $\eta'$  is 41% at the "optimum" target thickness of  $\sim 1.2 \times 10^{16}$   $D_2$  molecules/cm<sup>2</sup>, whereas at one-half that target thickness  $\eta'$  has only dropped to 34%. The loss in efficiency means a greater investment in power supplies, whereas the thinner target means a smaller gas load (less pumping)

and/or shorter neutralizer (smaller building). The neutral-beam designer must consider both to achieve the smallest overall cost of the system.

Although  $D^-$  beams look best at higher energies, no one has as yet produced sufficiently intense  $D^-$  beams to permit serious design considerations. The rest of the discussion will therefore deal with positive ion beams.

#### MIXED BEAMS

Designers and experimenters generally would prefer to have injectors providing neutral atoms at a single energy. As mentioned earlier, positive ions extracted from a deuterium (or hydrogen) plasma contain a mixture of  $D^+$ ,  $D_2^+$ , and  $D_3^+$  ( $H^+$ ,  $H_2^+$ ,  $H_3^+$ ) ions. Unwanted species can, in principle, be rejected at low energy by a magnetic selection process. However, to minimize space-charge blowup, present high-power-density beam systems have the neutralizer immediately following the last element of the accelerator system; consequently, no momentum selection is possible. The neutral beam is produced from collisions of all three primary ions and their collision products with the neutralizer gas (see Fig. 2), and a realistic analysis requires a knowledge of the ion-species composition of the extracted beam.

Unfortunately, there are few reliable measurements of beam compositions from high-power sources, and detailed experimental data on the interdependence of ion-species mixture, gas flow, arc voltage and current, electron temperature, wall material and temperature, and ion current density are badly needed. For the present purpose, we use as examples two species-mixtures measured with different operating conditions in high-current sources,  $D^+:D_2^+:D_3^+ = 60:20:20$  and  $75:15:10$ ,<sup>(3)</sup> and a hypothetical mixture,  $90:7:3$ .

In Figures 5-10 we show power-flow diagrams for six different experimental conditions that all yield 1 MW of 120-keV H or D beams. Figures 5-10 are for "optimum"

neutralizer thicknesses, as defined in the previous section.

Figures 5-7 show the effect of changes in the deuterium ion-species composition.

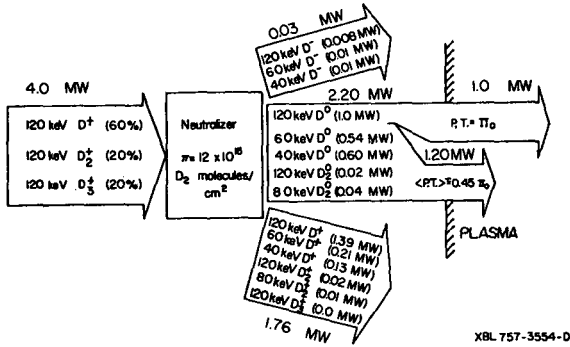


FIGURE 5

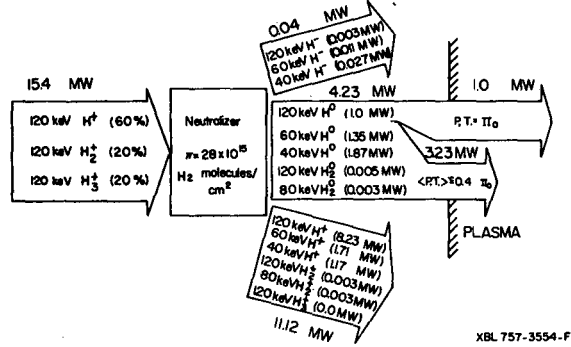


FIGURE 8

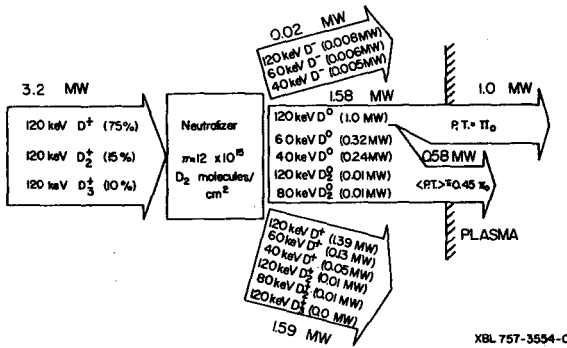


FIGURE 6

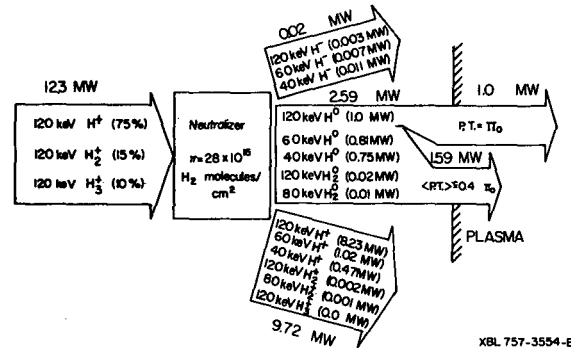


FIGURE 9

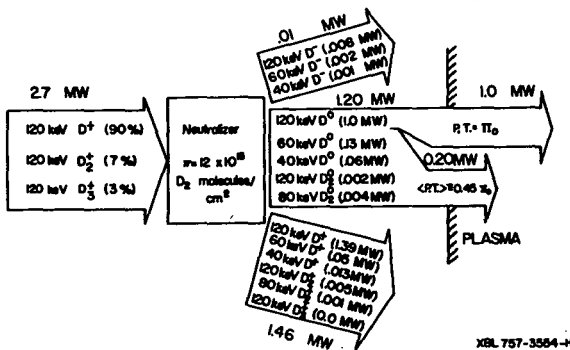


FIGURE 7

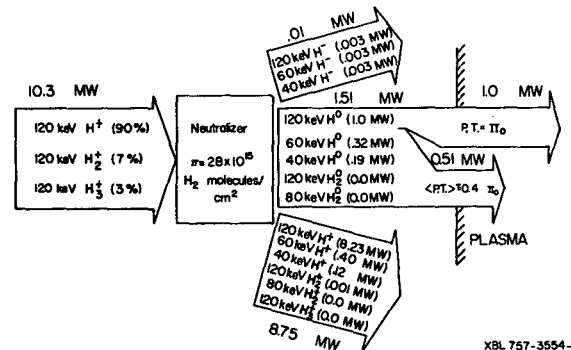


FIGURE 10

FIGURES 5-10. Power-flow diagrams for 1 MW, 120 keV D<sup>0</sup> and H<sup>0</sup> injection systems, for three initial deuterium-ion-species compositions and three equivalent hydrogen-ion-species compositions, at "optimum" neutralizer target-thicknesses (see text).

We see that a change in the  $D^+$  component from 60% to 90% decreases the net power requirement by 40% and the lower-energy neutral beam component by a factor of six.

Figures 8-10 are similar flow charts for hydrogen beams, which might be used in a large experimental device to provide the proper plasma penetration without introducing radioactivity problems. The neutralization efficiencies are very low for all three cases, the neutralizers must be longer, and the technical problem of handling the waste energy from the residual ion beams is huge. Without direct energy recovery, this kind of operation is very unattractive.

Figure 11 is to be compared with Figure 6; the difference is that the neutralizer thickness in Figure 11 is one-half the value in Figure 6. The designer might choose this option because the length of the beam line (neutralizer) could be reduced about 30%. The price is a 25% increase in input power (most of which must be handled by the residual-ion-beam dump), and a larger pumping speed caused by the higher conductance of the neutralizer.

We note that although the power in the negative ion beams is small on a percentage

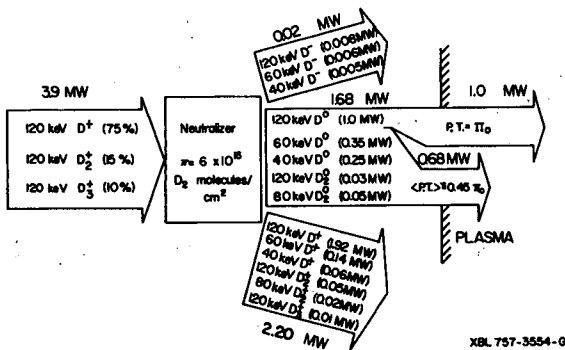


FIGURE 11. Power-flow diagram for the species mix 75%  $D^+$ , 15%  $D_2^+$  and 10%  $D_3^+$  for a 1 MW, 120 keV  $D^0$  injection system at one-half the "optimum" neutralizer target-thickness.

basis, it must be taken into account when siting cryopanel etc. in the beam lines.

The previous examples have shown the advantages of increasing the atomic-ion population. Figure 12 shows that there is an energy above which the energy of molecular ions is converted to neutrals more

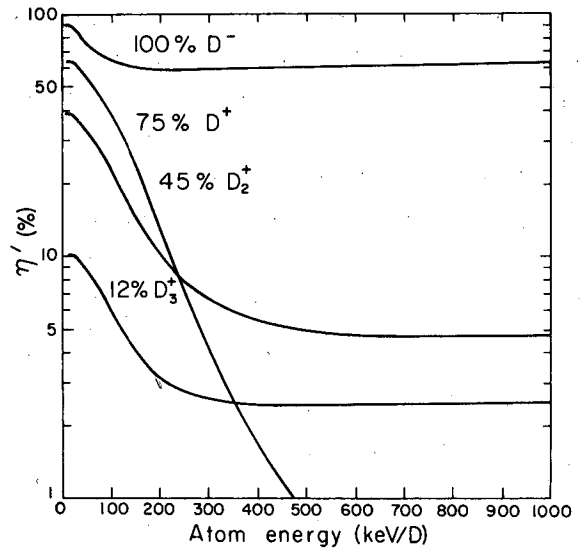


FIGURE 12. Neutralization efficiency,  $\eta'$ , (see equation [2]) vs the resultant deuterium-atom energy for beams of 75%  $D^0$  or 45%  $D_2^+$  or 12%  $D_3^+$  with the remainders of each beam in other ions.

efficiently than energy in atomic ions. The examples of ion concentrations shown have been observed experimentally. The drawback is that a system optimized for  $D_2^+$  must have twice the  $D^+$ -system accelerator voltage. As always,  $D^-$  beams, if obtainable, are preferable to positive-ion beams.

DIRECT RECOVERY

One possibility for improving the neutralization efficiency for neutral beams produced from mixed-species positive-ion beams is to couple in an energy-recovery device.<sup>(7)</sup> In Figures 13-15 we show the effect of energy recovery with 80, 90, 95, and 100% efficiency on the neutralization efficiency  $\eta'$ . The three figures are for various  $D^+$ :  $D_2^+$ :  $D_3^+$  mixtures -- 60:20:20 (Figure 13)

and 75:15:10 (Figure 14) are indicative of the range of measured beams; 90:7:3 (Figure 15) is an, as yet, unachieved mix and is shown here to stress the importance of development efforts to improve the  $D^+$  fraction of the beams. For these figures it is assumed that all ions are recovered with the indicated efficiency. Note that at 120 keV (the TFTR injection energy) the neutralization efficiency can be increased by more than 50% even with a recovery efficiency of only 80%. At the higher energies it will be extremely important to not only attain

the highest possible recovery efficiency but also to maximize the  $D^+$  composition of the beams. Above  $\sim 300$  keV positive ions are not efficiently neutralized even for the most optimistic combination of  $D^+$  enhancement and recovery efficiency (Figure 15).

The assumption that the energy of all ions can be recovered may be optimistic. In Figure 16 we show the efficiency for one particular set of parameters (75%  $D^+$ , 15%  $D_2^+$ , 10%  $D_3^+$  with 90% energy-recovery efficiency) for the case in which the energy of

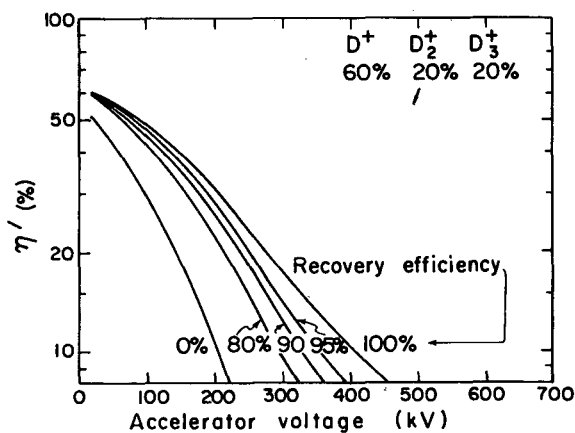


FIGURE 13

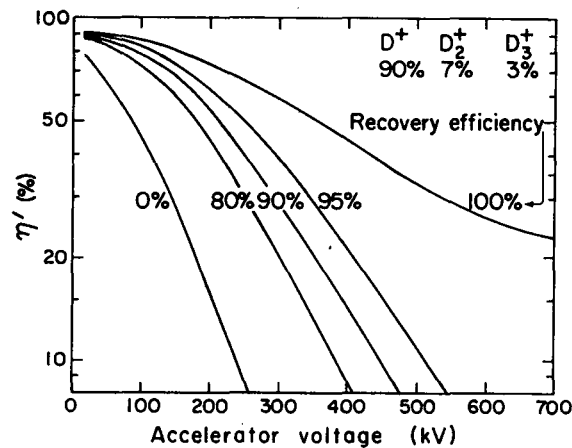


FIGURE 15

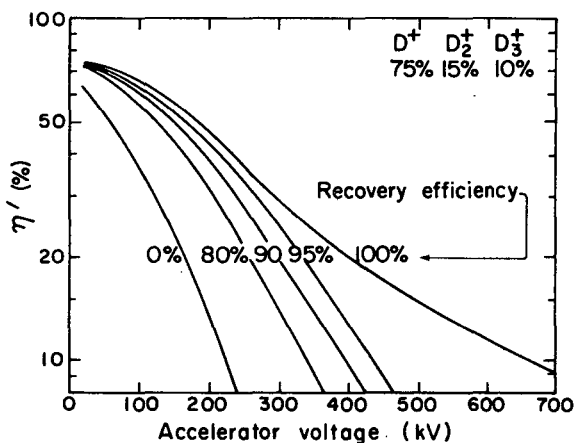


FIGURE 14

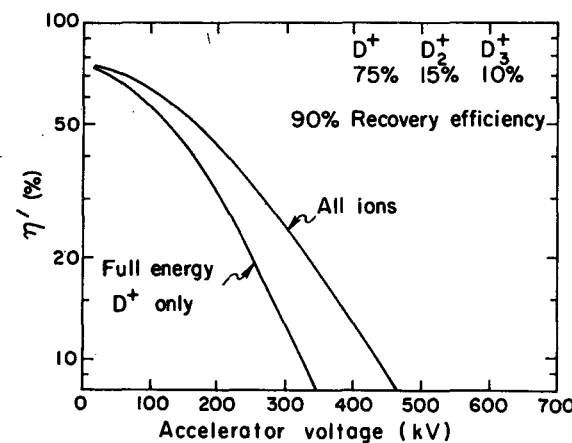


FIGURE 16

FIGURES 13-16. "Optimum" neutralization efficiency,  $\eta'$ , for full energy  $D^0$  atoms (see equation [2]) vs accelerator voltage for the  $D^+ : D_2^+ : D_3^+$  mixtures shown, assuming charged-particle-recovery efficiencies of 100%, 95%, 90%, and 80%. The curve with no recovery is also shown for comparison. In Fig. 16, the effect of recovering only the full-energy  $D^+$  ions is compared with that of recovering the energy of all ions with 90% efficiency.

all ions is recovered and the case in which only the energy of the "full-energy"-D<sup>+</sup> ions is recovered. The difference in  $\eta'$  is quite pronounced. This figure again emphasizes that our examples in this paper are only illustrative for generalized injection systems. A specific system must be evaluated for the specific parameters relevant to that system.

#### DISCUSSION

Negative deuterium-ion beams, if they can be achieved with good efficiency and good optics, will minimize the designers' problems. Increasing the atomic-ion component of positive-ion beams can be of great importance; we believe that a much larger experimental effort is called for in this area.

There is no experience, at this writing, with high-power beams at energies above 40 keV. In addition, the experimental data concerning ion-composition vs pressure, arc current, etc. are often contradictory and too meager to allow a designer to make optimized plans.

Even the uncertainties in the atomic-collision processes are large enough to

have a considerable effect on performance and costs. The neutral beam data base is too small to permit calculations of optimized designs at this time.

#### ACKNOWLEDGMENT

We thank C. F. Chan for his contributions to the development of the computer code used in this work.

#### REFERENCES

1. TFTR Final Conceptual Design Report, PPPL-1275, PH-R-001, (1976).
2. MX Major Project Proposal, Lawrence Livermore Laboratory, LLL-Prop-142, (1976).
3. K. H. Berkner, R. V. Pyle, and J. W. Stearns, Nucl. Fusion **15**, 249 (1975).
4. TFTR Neutral Beam Injection System Conceptual Design, Lawrence Berkeley Laboratory, Rept. LBL-3296 (1975).
5. S. K. Allison and M. Garcia-Munoz in Atomic and Molecular Processes, D. R. Bates, ed., Academic Press (1962).
6. K. H. Berkner, T. J. Morgan, R. V. Pyle, and J. W. Stearns, Phys. Rev. **A8**, 2870 (1973).
7. See, for example, R. W. Moir, "A Review of Direct Energy Conversion for Fusion Reactor," Session X, this conference.

This report was done with support from the United States Energy Research and Development Administration. Any conclusions or opinions expressed in this report represent solely those of the author(s) and not necessarily those of The Regents of the University of California, the Lawrence Berkeley Laboratory or the United States Energy Research and Development Administration.

TECHNICAL INFORMATION DIVISION  
LAWRENCE BERKELEY LABORATORY  
UNIVERSITY OF CALIFORNIA  
BERKELEY, CALIFORNIA 94720